

# Scaling and precursor motifs in earthquake networks

Marco Baiesi\*

*INFM, Dipartimento di Fisica, Università di Padova, I-35131 Padova, Italy.*

(Dated: September 23, 2018)

A measure of the correlation between two earthquakes is used to link events to their aftershocks, generating a growing network structure. In this framework one can quantify whether an aftershock is close or far, from main shocks of all magnitudes. We find that simple network motifs involving links to far aftershocks appear frequently before the three biggest earthquakes of the last 16 years in Southern California. Hence, networks could be useful to detect symptoms typically preceding major events.

PACS numbers: 91.30.Px, 89.75.Hc, 91.30.Dk

A fundamental open issue in the field of seismicity is whether earthquakes are to some extent predictable or not [1]. There are conflicting points of view about this [1, 2]. Nevertheless, phenomenological approaches have been used for some decades to formulate algorithms for earthquake prediction [3, 4, 5, 6], sometimes based on the search for complex (long-range) correlations [3].

Insight into the issue of seismicity and maybe of earthquake prediction can be obtained by measuring the correlations between any pair of earthquakes. One method to estimate the amount of correlation was put forward in Ref. [7] (see also [8]), based on the statistical properties of earthquakes. If epicenters are distributed with a fractal dimension  $d_f$ , the mean number of events within an area of radius  $l$  should scale as  $l^{d_f}$ . According to the Gutenberg-Richter law [1], the number of these events with magnitude  $\geq m$  is proportional to  $10^{-bm}$ , with  $b \approx 1$ . Of course, the number of these events is on average also proportional to the time  $t$  we have been spending to record them. Hence, globally the mean number of events scales with the size of the space-time-magnitude window as  $n \simeq K t 10^{-bm} l^{d_f}$ , where  $K$  is a constant related to the seismic activity. When a new event  $j$  takes place, it defines a point of view from which one can assess whether past seismic events appear unusual or usual, with respect to their expected average number. Indeed, any pair of events  $(i, j)$ , separated by a time interval  $t_{ij}$  and a distance  $l_{ij}$ , defines an expected number of events  $n_{ij} = K t_{ij} 10^{-bm_i} l_{ij}^{d_f}$ , where  $m_i$  is the magnitude of the first event.

One finds small  $n_{ij}$  values when  $j$  occurs immediately after  $i$ , very close to  $i$ , and if  $i$  has a large magnitude. A very small  $n_{ij}$  value means that an event with magnitude  $m_i$  had very small probability to occur in the space-time window defined by event  $j$ . Since such a case should rarely take place at random, its actual occurrence tells us that  $i$  and  $j$  are correlated. Furthermore, the smaller is  $n_{ij}$ , the more unusual is event  $i$  “with respect to  $j$ ”, the more  $i$  and  $j$  are correlated [9], as it was argued in Ref. [7]. Hence, one can adopt  $n_{ij}$  as a metric for quantifying correlations between events. On the basis of  $n_{ij}$  one can also build a network of earthquakes [7] by

drawing an oriented link to a new event  $j$  only from the event  $i$  giving the smallest  $n_{ij}$  value (denoted as  $n_j^*$ ). In this pair, we call event  $i$  the “main shock” and  $j$  is the “aftershock” even if  $m_j > m_i$  [10].

In this Letter we examine such earthquake correlation graphs by means of tools of network theory. We show that the notion of distance at the basis of the network construction underlies remarkable statistical scaling properties, which should reflect basic mechanisms of earthquake formation and propagation. We also find that some simple motifs (small pieces composed by a few nodes and links [11]) could constitute an interesting kind of precursor of major events. The study of the motif occurrences is a strategy to understand the properties of the systems described by networks [11]. For example, it is currently believed that understanding the statistics of simple motifs in protein-protein interactions and transcription regulatory networks can help to understand the metabolism [11, 12].

The catalog we have analyzed is maintained by the Southern California (SC) Earthquake Data Center [13]. Data in the period ranging from the 1st of January 1984 to the 31st of December 2003, and earthquakes with magnitude  $m \geq m_{\leq} = 3.0$  are considered (8858 events). In the area covered by the catalog the Gutenberg-Richter law holds with  $b \simeq 0.95$  [14], and  $d_f = 1.6$  [15]. Quantities are always measured in MKS units.

We examine the three-dimensional distribution of earthquakes, taking into account their epicenters (latitude and longitude) and depths, i.e., their hypocenters. The spatial separation between events is given by the Euclidean distance between their hypocenters, and the fractal dimension of hypocenters is supposed to be  $D_f = 1 + d_f = 2.6$ . The metric we use is then  $n_{ij} = K' l_{ij}^{D_f} 10^{-bm_i} t_{ij}$ . Links reliably denoting correlations have  $n_{ij} \leq n_c$ , with a suitable threshold  $n_c$  [7, 16]. In order to define a selection procedure independent of the constant  $K'$ , here we use  $n_c = \langle n^* \rangle / 10$ , where  $\langle n^* \rangle$  denotes the average of all  $n_i^*$  with  $i = 2, 3, \dots, j - 1$ .

If at most one incoming link per node is allowed, the network has the form of a growing tree [7]. We relax this constraint because we want a richer network structure,

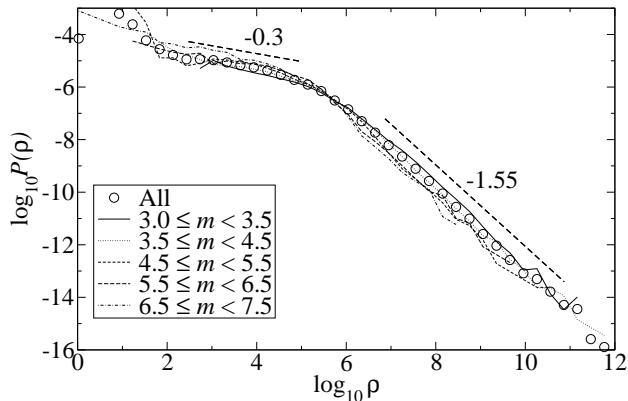


FIG. 1: Log-log plot of the global distribution  $P(\rho)$  (circles), and of the distributions  $P_{[m_1, m_2]}(\rho)$  generated by earthquakes with magnitude in ranges  $[m_1, m_2)$  (see legend). Two power-law regimes (with relative exponents) are evidenced by dashed straight lines.

with abundance of motifs like triangles of linked nodes, which are usually associated with the presence of non-trivial correlations within networks [17]. Nearly optimal incoming links to a new event have  $n_{ij}$  slightly greater than their minimum value  $n_j^*$  and are the first candidates to be added to the tree structure: hence, we choose to draw a link when  $n_{ij} \leq n_c$  and  $n_{ij} \leq \phi n_j^*$ , with constant  $\phi > 1$  (this procedure is also suggested by the fact that data from catalogs have experimental errors). We set  $\phi = 10$ , obtaining roughly 2 outgoing links per node, but other similar values do not considerably alter the results.

Our analysis of the precursor phenomena is based on the statistics of the quantity

$$\rho_{ij} = l_{ij}^{D_f} 10^{-b m_i}, \quad (1)$$

which is the space-magnitude part of the metric values  $n_{ij}$  associated with drawn links. In Fig. 1 we show its distribution  $P(\rho)$ . In addition, we also plot the distributions of  $\rho$  relative to links departing from shocks in ranges of magnitudes  $[m_1, m_2)$ , denoted as  $P_{[m_1, m_2]}(\rho)$ . Two distinct power laws appear in  $P(\rho)$  as well as in all  $P_{[m_1, m_2]}(\rho)$  considered. For  $\rho \rightarrow 0$ ,  $P(\rho) \sim \rho^{-\alpha}$ , with  $\alpha \simeq 0.3$ . In the regime  $\rho \rightarrow \infty$  instead  $P(\rho) \sim \rho^{-\beta}$ , with  $\beta \simeq 1.55$ . Since all  $P_{[m_1, m_2]}(\rho)$  are quite well overlapped, and the aftershock distances vary weakly with time after an event (not shown), a length  $l_m = \rho^{1/D_f} = 10^{(b/D_f)m}$  is a good unit for measuring the distance of aftershocks from an event of magnitude  $m$ . Thus, the exponent  $\sigma = b/D_f \simeq 0.37$  might justify the rescaling of aftershocks distances with a factor  $10^{\sigma m}$ , as it was done in Ref. [7] ( $\sigma \simeq 0.4$  there).

The distributions  $P(\rho)$  describes a property of individual correlations between pairs of earthquakes, from which we clearly see that two classes of aftershocks exist, corresponding to the two regimes of  $P(\rho)$ . A geophysical explanation of these two regimes could be related to

the hierarchical fault structure: possibly, small  $\rho$  are connected to the conventional aftershocks within the rupture area, while the high  $\rho$  region could be determined mainly by inter-fault aftershocks, which are also detected by our method.

A wide area of aftershock activity, as quantified by a large  $\rho$  value, may be favored by high stresses within the crust, and hence may be related to the periods prior to strong earthquakes. During these periods, it is also reasonable to find complex correlations in the stress field [18]. We have tested the possibility that these phenomena are highlighted by peculiar network motifs, i.e., by studying the local topological structure of the growing network of earthquakes. Indications supporting our hypothesis can be found by modifying the notion of local clustering coefficient of a node, which is normally given by the fraction of triangles it forms with its neighbors [17]. In order to meet our former requirements, the motifs we study here are special triangles (ST), in which the  $\rho$  value carried by the first link ( $i$ - $k$  link in the Inset of Fig. 2) is larger than a given threshold  $\rho_0$ . The special clustering coefficient of a new node  $j$  is then  $C_j = \Delta_j / \Delta_j^{\max}$ , where  $\Delta_j$  is the number of ST it forms with its  $\kappa_j$  main shocks, and  $\Delta_j^{\max} = \kappa_j(\kappa_j - 1)/2$ . By definition  $C_j = 0$  if  $\kappa < 2$ .

To show that ST may be precursors of strong events we proceed as follows: The first three years of the catalog are used to obtain an initial estimate of  $\langle n^* \rangle$ . During the next year we just add links, to avoid possible problems arising from the analysis of a network where links to old events are lacking. Then, from the beginning of 1988, an algorithm analyzes the signal given by the  $C$  value, evaluated for each event when it takes place. When  $C > 0$ , we start an integration of the  $C$  signal, called  $C_I$ , which is reset to zero if  $C = 0$  for a period  $T_0$ . Values  $T_0 = 60$  days and  $\rho_0 = 10^7$  yield a reasonable overall rate of  $C > 0$  values (spikes  $0 < C \leq 1$  in Fig. 2), avoiding the saturation of  $C_I$ , which is the signal that we think is somewhat proportional to the seismic hazard in the region. The periods when  $C_I$  is greater than a constant threshold  $C_H = 3$  are declared as alarms.

Figure 2 suggests that there is a relation between alarm times and the occurrence of the three biggest events in the catalog: for Landers event [ $m = 7.3$ , labeled with (A)], alarm would have started 9 weeks before its occurrence, for Northridge [(B),  $m = 6.7$ ] one had to wait 6 weeks after the declaration of the alarm, while the alarm before Hector Mine [(C),  $m = 7.1$ ] started 10 weeks in advance. Thus, they would have been predicted in the short term. The San Simeon event [(D),  $m = 6.5$ ] instead was not within an alarm time, while an alarm was also declared in a period when the biggest event had  $m = 5.7$ .

The spatial location of the precursor motifs is another interesting issue. Fig. 3 and Fig. 4 show the distribution of ST giving rise to the alarms (i.e. when  $C_I > 0$ ) before the three biggest events. In Fig. 3, small letters

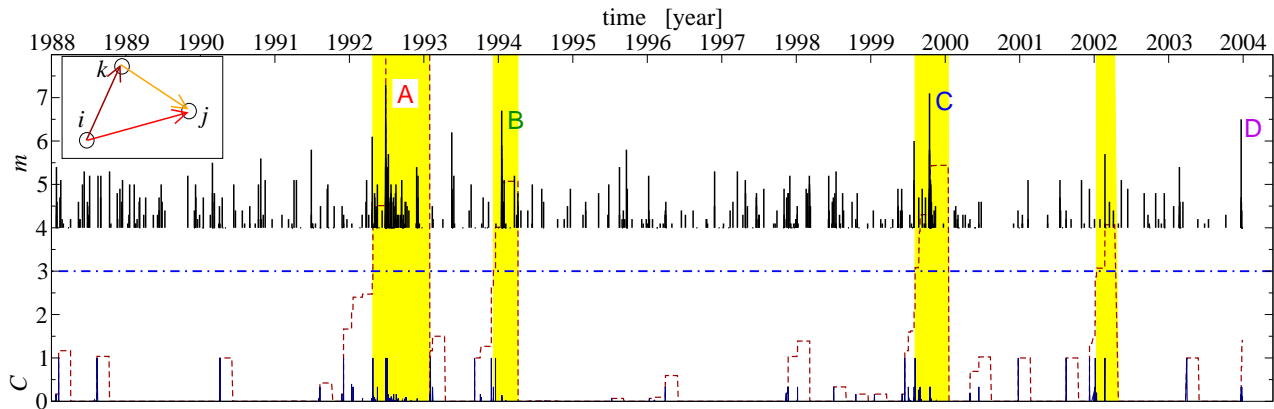


FIG. 2: (Color online) Time series of event magnitudes (above, only  $m \geq 4$  are shown) and of special clustering  $C$  of events (below). Landers (A), Northridge (B), Hector Mine (C), and San Simeon (D) are the four biggest events since 1988 in the catalog. The integrated signal  $C_I$  is shown as a dashed line, while the horizontal dot-dashed line represents the threshold value  $C_H = 3$ : when  $C_I > C_H$ , alarms are declared (shaded areas, yellow online). Inset: sketch of a triangle of linked events, which is “special” if  $\rho_{ik} > \rho_0$ .

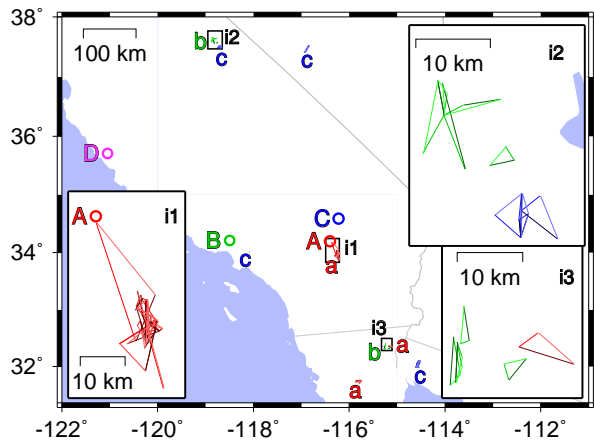


FIG. 3: (Color online) Location of big events (circles, same capital letters discussed in the text and in Fig. 2), and of precursor patterns (ST), marked with the same letter (and color online) of the relative big shock. The three insets are enlargements of areas with ST. Color tones of the three links in a triangle follow the same order as in the Inset of Fig. 2; in particular the older link is darker.

corresponding to the big event ones denote areas with ST, and three insets show enlargements of some of them. Excluding a cluster of ST which would have indicated the future location of Landers epicenter [Fig. 3(i1)], ST do not appear close to the location of the incoming big events, in agreement with the idea that the preparation of an earthquake is not localized around its future source (see [3] and references therein).

A plausible explanation of both this delocalization of the precursor patterns with respect to the big shock and the relation between high  $\rho$  values and strong earthquakes might come from the critical point scenario [18, 19], in which a big event represents a finite time singularity [20]. Indeed, as in the theory of critical phe-

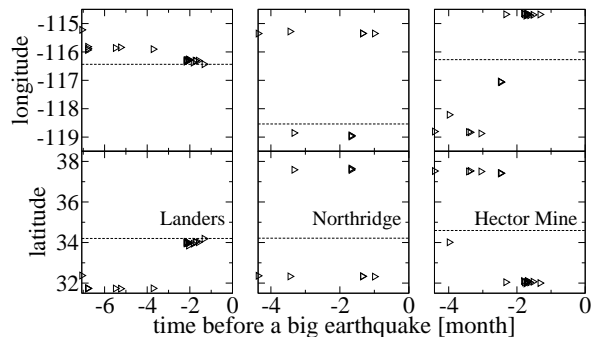


FIG. 4: Longitude and latitude of the last node of ST, during the period when  $C_I > 0$  before Landers, Northridge and Hector Mine events. The coordinates of the big events are plotted as dashed lines. There is a clear convergence of the ST to the Landers epicenter [see also Fig 3(i1)].

nomena, a suitably defined correlation length shows a singular behavior diverging prior to big earthquakes [5, 21]. This length is evaluated by a procedure which sums the distances between events which are not aftershocks. Due to our results, we believe that aftershock distances may be a complementary indicator of long range correlations, and in particular that relatively far aftershocks could be a typical symptom of an incoming strong earthquake. Notice that we obtain useful informations also from the statistics of the aftershocks of the numerous minor earthquakes, in agreement with the idea that the latter are active players in seismicity [22].

To assess the stability of our simple algorithm, in Fig. 5 we have plotted an error diagram [23] where the fraction of events with  $m \geq m_>$  that are not predicted is shown as a function of the fraction of alarm time. In the diagram, the performance of a random alarm declaration is represented by a line joining the point (0, 1) with (1, 0).

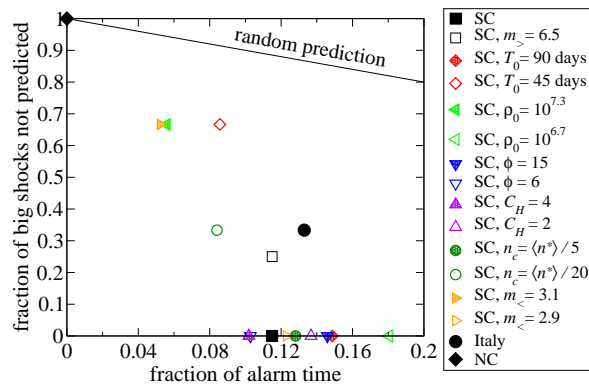


FIG. 5: (Color online) Error diagram. Symbols are associated with geographic zones and eventually with a modified parameter (see text). The line represents the performance of a random alarm declaration.

Starting from the point ( $n_c = \langle n^* \rangle / 10$ ,  $\phi = 10$ ,  $\rho_0 = 10^7$ ,  $C_H = 3$ ,  $T_0 = 60$  days,  $m_< = 3.0$ ,  $m_> = 6.7$ ) in the parameter space, we have varied one of the parameters per time, around its initial point, and plotted the relative performance in Fig. 5. One clearly see that the algorithm does better than a random alarm declaration, and that it is reasonably stable.

The case illustrated in this paper shows that a translation of issues of seismicity into a network problem can be a fruitful approach. In order to have further insight on this possibility, we have analyzed two other catalogs, centered around Northern California (NC) and Italy [24], and covering the same time span of our SC catalog. We have used the same parameters of SC, but for NC we set  $m_> = 6.5$  to include both S. Simeon and Loma Prieta (1989,  $m = 7$ ) events in the big shock list. The algorithm does not recognize any of the two NC big events (no alarms declared, see Fig. 5). In Italy we set  $\rho_0 = 10^8$  and a shift of the magnitudes ( $m_< = 2.5$ ,  $m_> = 5.8$ ) is necessary in order to include the two largest events (Umbria 1997,  $m = 6$  and Molise 2002,  $m = 5.9$ ) in the big shock list and a considerable number of smaller ones in the analysis. In this case, 4/6 of the big events are predicted, including the two most disruptive ones, with a fraction of alarm time  $\approx 0.13$ , as shown in Fig. 5.

In summary, by means of an appropriate metric quantifying the amount of correlation between earthquakes, aftershocks of any event can be identified. Aftershock distances from a shock of magnitude  $m$  are properly measured by a length unit scaling as  $10^{0.37m}$ . This information has been combined with a study of the local topology of the growing network of earthquakes, to show that simple motifs embodying links to unusually far aftershocks appeared frequently before Landers, Northridge and Hector Mine events in Southern California.

The author thanks A. Kabakçioğlu, E. Orlandini, M. Paczuski and A. L. Stella for the useful comments and discussions. Support from INFM-PAIS02 is acknowl-

edged.

- 
- \* Electronic address: baiesi@pd.infn.it
- [1] C. H. Scholz, *The Mechanics of Earthquakes and Faulting* (Cambridge University Press, Cambridge, 2002), 2nd ed.
  - [2] Nature (1999), "Is the reliable prediction of individual earthquakes a realistic scientific goal?", see the web page <http://www.nature.com/nature/debates/index.html>.
  - [3] V. Keilis-Borok, *Annu. Rev. Earth Planet. Sci.* **30**, 1 (2002).
  - [4] V. I. Keilis-Borok, P. N. Shebalin, and I. V. Zaliapin, *Proc. Natl. Acad. Sci. USA* **99**, 16562 (2002).
  - [5] I. Zaliapin, Z. Liu, G. Zöller, V. Keilis-Borok, and D. Turcotte, *Comp. Seism.* **33**, 141 (2002).
  - [6] V. Keilis-Borok, P. Shebalin, A. Gabrielov, and D. Turcotte (2003), e-print physics/0312088.
  - [7] M. Baiesi and M. Paczuski, *Phys. Rev. E* **69**, 066106 (2004).
  - [8] M. Baiesi and M. Paczuski (2004), physics/0408018.
  - [9] This way of thinking is rather general and can be applied to contexts different from seismicity as well.
  - [10] As discussed in [7], the standard aftershock collection instead would count all events following a stronger earthquake, in a given time window and far less than a maximum distance.
  - [11] R. Milo et al., *Science* **298**, 824 (2002).
  - [12] E. Ziv, R. Koytcheff, and C. Wiggins (2003), e-print cond-mat/0306610; S. Wuchty, Z. N. Oltvai, and A. L. Barabási, *Nature Genet.* **35**, 176 (2003); E. Yeger-Lotem et al., *Proc. Natl. Acad. Sci. USA* **101**, 5934 (2004); M. Middendorf et al. (2004), e-print q-bio.MN/0402017.
  - [13] <http://www.data.scec.org/ftp/catalogs/SCSN/>
  - [14] P. Bak, K. Christensen, L. Danon, and T. Scanlon, *Phys. Rev. Lett.* **88**, 178501 (2002).
  - [15] A. Corral, *Phys. Rev. E* **68**, 035102(R) (2003).
  - [16] In order to avoid too long links between nearly simultaneous far events, a minimum time interval  $t_{\min} = 60$  s between two events is imposed. In the metric, a minimum distance  $l_{\min} = 100$  m is also used.
  - [17] D. J. Watts and S. H. Strogatz, *Nature* **393**, 440 (1998); R. Albert and A.-L. Barabási, *Rev. Mod. Phys.* **74**, 47 (2002); S. N. Dorogovtsev and J. F. F. Mendes, *Adv. Phys.* **51**, 1079 (2002).
  - [18] S. C. Jaumé and L. R. Sykes, *Pure Appl. Geophys.* **155**, 279 (1999).
  - [19] L. R. Sykes and S. C. Jaumé, *Nature* **348**, 595 (1990); C. G. Bufe and D. J. Varnes, *J. Geophys. Res.* **98**, 9871 (1993); D. D. Bowman, G. Ouillon, C. G. Sammis, A. Sornette, and D. Sornette, *J. Geophys. Res.* **103**, 24,359 (1998); D. D. Bowman and G. C. P. King, *Geophys. Res. Lett.* (2001).
  - [20] C. G. Sammis and D. Sornette, *Proc. Natl. Acad. Sci. USA* **99**, 2501 (2002).
  - [21] G. Zöller, S. Hainzl, and J. Kurths, *J. Geophys. Res.* **106**, 2167 (2001); G. Zöller and S. Hainzl, *Geophys. Res. Lett.* **29**, 53 (2002).
  - [22] A. Helmstetter, *Phys. Rev. Lett.* **91**, 058501 (2003).
  - [23] G. M. Molchan, *Pure Appl. Geophys.* **149**, 233 (1997).
  - [24] <http://quake.geo.berkeley.edu/anss/catalog-search.html>